Astronomy & Astrophysics manuscript no. 5456AAL February 5, 2008
(DOI: will be inserted by hand later)

arXiv:astro-ph/0607229v1 11 Jul 2006

Swift, RXTE, and INTEGRAL observation of Swift J1922.7-1716

M. Falanga[1,2,⋆], T. Belloni[3], S. Campana[3]

[1] CEA Saclay, DSM/DAPNIA/Service d'Astrophysique (CNRS FRE 2591), F-91191, Gif sur Yvette, France
[2] Unité mixte de recherche Astroparticule et Cosmologie, 11 place Berthelot, 75005 Paris, France
[3] INAF - Osservatorio Astronomico di Brera, Via Bianchi 46, 23807 Merate, Italy

the date of receipt and acceptance should be inserted later

Abstract.
We report the results of analyzing *Swift*, *RossiXTE*, and *INTEGRAL* data of Swift J1922.7-1716, a likely transient X-ray source discovered by Swift/BAT. Both the fast variability measured by the *RXTE*/PCA and the combined *Swift*/XRT, *RXTE*/PCA, and *INTEGRAL*/ISGRI (0.5–100 keV) energy spectrum suggest that the system is a neutron-star low-mass X-ray binary or a black-hole candidate at low accretion levels. The non-simultaneous spectra are consistent with the same spectral shape and flux, suggesting little variability over the period July to October 2005, but the analysis of archival *INTEGRAL* data shows that the source was not detected in 2003–2004, suggesting a transient or strongly variable behavior.

Key words. binaries: close – stars: individual (Swift J1922.7-1716)

1. Introduction

Swift J1922.7-1716 was discovered during the *Swift* Burst Alert Telescope (BAT) hard X-ray survey. The BAT survey covers the 15–200 keV band and the time range December 2004 - March 2005 where Swift J1922.7-1716 was reported as $> 5.5\sigma$ detection (Tueller et al., 2006a,b). The BAT detection was also confirmed in a follow-up observation with the *Swift* X-ray telescope (XRT) in the 0.5–10 keV energy band. The source was found at the best-fit position $\alpha_{\rm J2000} = 19^{\rm h}22^{\rm m}37\overset{\rm s}{.}0$ and $\delta_{\rm J2000} = -17^\circ17'02\overset{''}{.}6$ with an estimated uncertainty of $3\overset{''}{.}2$ (90% confidence). From the Ultra-Violet Optical Telescope (UVOT) onboard *Swift*, the observed counterpart was not consistent with the Palomar survey (Tueller et al., 2006b). Using the XRT data, the source spectrum was consistent with an absorbed power-law model with a photon index of $\Gamma = 2.05 \pm 0.05$ and a relatively low equivalent hydrogen column density $N_H = (1 \pm 0.5) \times 10^{21}$ cm^{-2} (Tueller et al., 2006a,b).

Swift J1922.7-1716 was also observed as a target of opportunity (ToO) performed on October 21, 2005 with the *Rossi X-ray Timing Explorer* (*RXTE*), and the data were made publicly available. The source was also detected serendipitously during the *International Gamma-Ray Astrophysics Laboratory* (*INTEGRAL*) ToO observation of HETE J1900.1-2455 performed from November 10–12, 2005. In this letter we report the result of the spectral and timing analysis of Swift J1922.7-1716 using the *Swift*, *RXTE*, and *INTEGRAL* data. We analyze the broad band spectrum from 0.5–100 keV and perform a timing analysis to identify the nature of this new source.

2. Observations and data

2.1. *Swift*

Swift carried out two observations of Swift J1922.7-1716 on July 8, 2005 and October 1, 2005. The XRT (Burrows et al. 2005) collected 6128 s data and 8215 s data in photon counting mode, respectively. The high source-count rate (~ 2 cts s^{-1}) is such that the source is piled-up. We analyzed these data by extracting products from an annulus with an inner radius of 5 pixels (11.8″) and outer radius 40 pixels (94.3″), where extracted 7468 counts and 10401 counts, respectively. The background within the extraction region is negligible ($< 1\%$).

For the spectral analysis, we generated appropriate ancillary response files with the FTOOL task `xrtmkarf`. Data were grouped to have 50 counts per energy channel. The calibrated energy range is 0.5–10 keV using v.7 of response files.

2.2. *RXTE*

We used publicly-available data from the proportional counter array (PCA; 2–60 keV) (Jahoda et al., 1996) and the High Energy X-ray Timing Experiment (HEXTE; 15–250 keV) (Rothschild et al., 1998) onboard the *RXTE* satellite. Swift J1922.7-1716 was observed on October 21,

---

Send offprint requests to: M. Falanga

[⋆] e-mail: `mfalanga@cea.fr`

2005 for two satellite orbits, from 08:54 UT for a total exposure time of 6.2 ks. For the spectral analysis, we extracted the PCA and HEXTE energy spectrum using the standard software package FTOOLS version 6.0.2. However, the HEXTE detection, with a count rate of ∼ 1.82 cts/s/cluster, was inadequate in this case for yielding a useful high-energy spectrum; therefore, it was excluded from the analysis. For the PCA, we limited the spectral and timing analysis using only the PCU2 data, which was on during the whole observation.

2.3. INTEGRAL

The present data was obtained during the *INTEGRAL* (Winkler et al., 2003) ToO observation starting on October 27, 2005 and ending on October 29, for a total exposure time of 210 ks. The observation, aimed at HETE J1900.1-2455, consists of 64 stable pointings with a source position offset between 7° and 11°. We used data from the coded mask imager IBIS/ISGRI (Ubertini et al., 2003; Lebrun et al., 2003) in the 20 to 200 keV energy range. The JEM-X monitor (Lund et al., 2003) was not used since the source was outside the field of view for all pointings. Data reduction was performed using the standard Offline Science Analysis (OSA) version 5.1. The algorithms used for the spatial and spectral analyses are described in Goldwurm et al. (2003). The ISGRI light curves are based on events selected according to the detector illumination pattern for Swift J1922.7-1716. We used an illumination factor threshold of 0.6 for the energy range 18–40 keV. In addition, we analyzed publicly-available ISGRI data from March 2003 to October 2004, for a total exposure time of 420 ks. In these data the source was not detected at a statistically significant level in the 20–60 keV energy band.

3. Results

3.1. ISGRI imaging and light curve

In order to study the *INTEGRAL* light curve and spectrum of Swift J1922.7-1716 we first deconvolved and analyzed the 64 single pointings separately and then combined them into a total mosaic image in the 20–40 keV energy band. In the mosaic, Swift J1922.7-1716 is clearly detected at a significance level of 16σ. The source was detected with the imaging procedure at the best-fit position $\alpha_{\rm J2000} = 19^{\rm h}22^{\rm m}36\overset{\rm s}{.}2$ and $\delta_{\rm J2000} = -17^\circ16'18\overset{''}{.}7$. This position, offset with respect to the *Swift*/XRT positions (Tueller et al., 2006a,b), is $0\overset{'}{.}44$. The 90% confidence error on the ISGRI coordinates (see Gros et al., 2003) is $1\overset{'}{.}1$. The background-subtracted 20–40 keV band light curve was extracted from the images using all available pointings, each with a ∼ 3.3 ks exposure. The source mean-count rate was almost constant at ~ 0.9 cts s^{-1} ($\sim 5.6 \times 10^{-11}$ erg cm^{-2} s^{-1}). The count rates are converted to flux using the spectrum model 4 described in Sect. 3.3.

3.2. Timing analysis

We searched for coherent pulsations over a wide range of periods (2ms–1000s) in the total PCA energy range without finding any significant signal. We derived the upper limits on the pulsed fraction for a sinusoidal modulation (semi-amplitude of modulation divided by the mean source count rate) at a 3σ confidence level (see Israel & Stella, 1996, for details of the algorithm used). For periods longer than about 10s, we are not sensitive to any pulsations due to the intrinsic aperiodic variability of the source. Upper limits in the 10%–4%, 3%–4%, and 4%–5% have been obtained for the 7s–1s, 1s–2.5ms, and 2.5ms–2ms period intervals, respectively. Also, when using the longer observation but low-statistics ISGRI events data in the 18–40 keV band, no coherent pulsation, orbital period or type-I X-ray bursts were found.

The 3–15 keV PCA light curve shows strong variability, around 1.1×10^{-10} erg cm^{-2} s^{-1}, in the form of fast flares with an excursion of about a factor of three, with a typical duration of a few seconds (see upper panel of Fig. 1). We studied the power density spectrum (PDS) of Swift J1922.7-1716 using the high time-resolution PCA data. The PDS can be fitted with three zero-centered Lorentzian components, for a total fractional rms variability, integrated in the 0.001-10 Hz band, of ∼37%. The characteristic frequencies of the three Lorentzian (see Belloni, Psaltis & van der Klis, 2002) are 0.042 ± 0.009 Hz, 0.55 ± 0.07 Hz, and 5.5 ± 1.0 Hz, about one decade apart from each other (see Fig. 1). The high level of variability and the Lorentzian decomposition are similar to those observed in black-hole candidates (BHC) in their low/hard state and in a neutron-star (NS) low-mass X-ray binary system (LMXB) in their low-luminosity states (see e.g., Belloni et al., 2002).

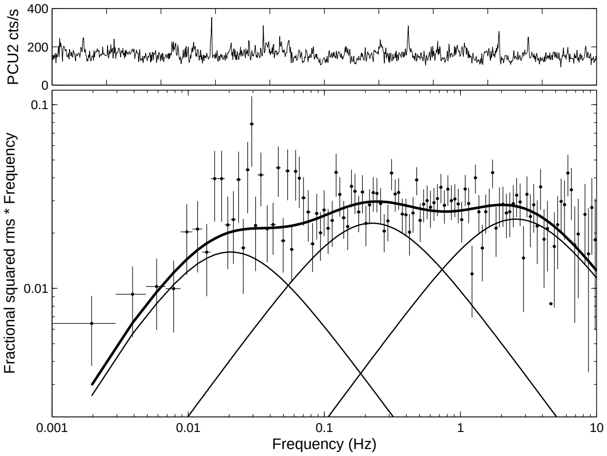

Fig. 1. Upper panel: the *RXTE*/PCA light curve of Swift J1922.7-1716 in the 3–15 keV energy band observed from 53664.37 to 53664.44 MJD. Lower panel: the power density spectrum in νP_ν form. The best fit Lorentzian models are also shown.

3.3. Spectral analysis

The spectral analysis was done using XSPEC version 11.3 (Arnaud, 1996) for the 0.5–7 keV *Swift*/XRT data, the 3–22 keV *RXTE*/PCA, and 20–100 keV *INTEGRAL*/ISGRI data. For the broad-band spectral analysis, a multiplicative factor for each instrument was included in the fit to take into account the uncertainty in the cross-calibration of the instruments, as well as variability across the non-simultaneous observations. The factor was fixed to 1 for the PCA data. All spectral uncertainties in the results are given at a 90% confidence level for single parameters.

First we fit the single data for each observation with a power-law (PL) model including for the Swift/XRT data a photoelectrically-absorbed blackbody (BB) model. We found that the spectral parameters are to the same order within the error range (see Table 1). We then fit the 0.5–100 keV broad-band spectrum using a simple photoelectrically-absorbed PL, model plus a BB, model for thermal soft emission below 3 keV and obtained a good χ^2/d.o.f. = 243/207. The best fit was found by replacing the PL with a cutoff PL model obtaining an χ^2/d.o.f. = 219/206. However, in our case, the PL multiplied by a high-energy exponential cutoff model provides a slightly better description of the data compared to the PL on the entire dataset at a 78% confidence level (estimated by means of an F-test). The best-fit values are found for a BB temperature, $kT_{\rm soft}$, of ~ 0.42 keV, a PL photon index of $\Gamma \sim 1.53$, and a cutoff energy of ~ 33 keV. The interstellar column density, $N_{\rm H}$, was found to be $\sim 0.14 \times 10^{22}$ cm^{-2}. This value is within the same order as the Galactic value, $N_{\rm H} = 0.12 \times 10^{22}$ cm^{-2}, reported in the radio maps of (Dickey & Lockman, 1990).

Assuming that the PL is due to Comptonization of soft photons by high-energy electrons, we replaced the phenomenological cutoff PL model with a more physical thermal Comptonization model. For this, we used the COMPTT model (Titarchuk, 1994), which is an analytic model describing the Comptonization of soft photons described by a Wien spectrum up-scattered in a hot plasma. The main model parameters are the Thomson optical depth $\tau_{\rm T}$ across the spherical or slab geometries, the electron temperature, $kT_{\rm e}$, and the soft seed photon temperature, $kT_{\rm seed}$. The soft thermal emission, $kT_{\rm soft}$ is fitted by a simple BB or a multi-temperature disc blackbody (DBB) model (Mitsuda et al., 1984). This model provides a good description of the data and the best-fit parameters are reported in Table 2.

We found that the DBB temperature, $kT_{\rm soft}$, and the soft seed photon temperature, $kT_{\rm seed}$, are within the same order, suggesting that the observed soft component is also the source of the seed photons. Therefore, we repeated the fit with $kT_{\rm soft} = kT_{\rm seed}$ and obtained only a marginally worse χ^2/d.o.f. = 226/206. In Fig. 2, we show the unfolded spectrum and the residuals of the data to the DBB plus COMPTT model. For the COMPTT model, assuming a spherical geometry instead of a slab/disc geometry leads to the same fit result. We tested for the presence of iron emission line, but neither a 6.4 keV iron line nor Compton reflection were significantly detected. The upper limit to the equivalent width for the iron line between 6.4 keV and 6.9 keV is 176 eV (90% confidence). For all the fits, the normalizations of the XRT, PCA, and ISGRI data were within 1.08 ± 0.03. Since Swift J1922.7-1716 was observed for *Swift*, *RXTE*, and *INTEGRAL* during different epochs, this probably indicates that the source flux did not vary across the different observations.

Table 1. Spectra fit for the single XRT, PCA, and ISGRI data.

Data set	XRT 1	XRT 2	PCA	ISGRI
Energy (keV)	0.5–7	0.5–7	3–22	22–100
Parameters	BB+PL	BB+PL	PL	PL
$N_{\rm H}$ (10^{21}cm^{-2})	$1.2^{+0.5}_{-0.4}$	$1.9^{+0.5}_{-0.5}$	–	–
$kT_{\rm soft}$ (keV)	$0.43^{+0.02}_{-0.02}$	$0.40^{+0.03}_{-0.03}$	–	–
$R_{\rm BB}$ (km)	13.4±0.4	$13.5^{+0.1}_{-0.1}$	–	–
Γ	$1.63^{+0.3}_{-0.4}$	$1.75^{+0.3}_{-0.4}$	$1.83^{+0.04}_{-0.04}$	$2.2^{+0.5}_{-0.6}$
χ^2/dof	89/88	83/82	21/25	10/9
$F_{\rm X}^{(a)}$	1.7	1.8	1.1	0.8

$^{(a)}$ unabsorbed flux in unit of 10^{-10}erg cm^{-1} s^{-1}.

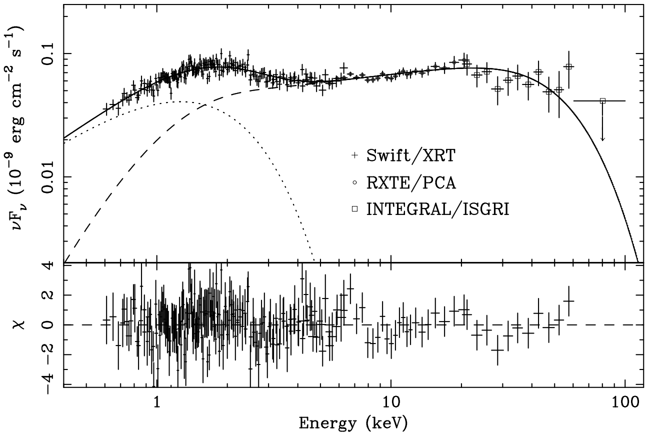

Fig. 2. The unfolded spectrum of Swift J1922.7-1716 fitted with an absorbed disc blackbody, DBB, plus COMPTT model. The data points correspond to the two XRT (0.5–7 keV), the PCA (4–22 keV), and the ISGRI (20–100 keV) spectra, respectively. The DBB model is shown by a dotted curve, the dashed curve gives the COMPTT model, while the total spectrum is shown by a solid curve. The lower panel presents the residuals between the data and the model.

4. Discussion and conclusions

The broad-band spectrum (0.5–100 keV) allowed us to perform an improved spectral analysis for the new source Swift J1922.7-1716 using the *Swift*/XRT, *RXTE*/PCA,

Table 2. Best-fit parameters of the XRT/PCA/ISGRI data.

Parameters	Model 1 BB+PL	Model 2 BB+CUTOFF PL	Model 3 DBB+CUTOFF PL	Model 4 BB+COMPTT	Model 5 DBB+COMPTT	Model 6 DBB+COMPTT
$N_{\rm H}$ (10^{21}cm^{-2})	$1.9^{+0.4}_{-0.3}$	$1.4^{+0.2}_{-0.4}$	$2.0^{+0.2}_{-0.2}$	$1.5^{+0.2}_{-0.2}$	$1.4^{+0.3}_{-0.2}$	$1.8^{+0.3}_{-0.2}$
$kT_{\rm soft}$ (keV)	$0.41^{+0.02}_{-0.02}$	$0.42^{+0.01}_{-0.03}$	$0.60^{+0.03}_{-0.03}$	$0.42^{+0.02}_{-0.02}$	$0.53^{+0.05}_{-0.04}$	$0.50^{+0.03}_{-0.03}$
$R_{\rm in}\sqrt{\cos i}$ (km)$^{(a)}$	–	–	$5.7^{+0.7}_{-0.5}$	–	$6.7^{+1.8}_{-1.3}$	8.9 ± 1.1
$R_{\rm BB}$ (km)	12.1 ± 0.9	12.5 ± 1.0	–	$15.7^{+1.5}_{-1.2}$	–	–
Γ	$1.8^{+0.4}_{-0.4}$	$1.43^{+0.13}_{-0.15}$	$1.43^{+0.13}_{-0.15}$	–	–	–
$E_{\rm cutoff}$ (keV)	–	32.5^{+17}_{-7}	28^{+15}_{-8}	–	–	–
$kT_{\rm seed}$ (keV)	–	–	–	$0.84^{+0.12}_{-0.16}$	$0.37^{+0.08}_{-0.16}$	$= kT_{\rm soft}$
$kT_{\rm e}$ (keV)	–	–	–	$10.7^{+3.2}_{-2.0}$	$10.7^{+3.3}_{-2.1}$	$10.6^{+3.3}_{-2.1}$
$\tau_{\rm T}$	–	–	–	$3.04^{+0.46}_{-0.54}$	$3.04^{+0.47}_{-0.52}$	$3.06^{+0.48}_{-0.51}$
χ^2/dof	243/207	219/206	232/206	211/205	219/205	226/206
$F^{(b)}_{0.1-100\rm keV}$	3.6×10^{-10}	3.7×10^{-10}	3.9×10^{-10}	3.3×10^{-10}	3.6×10^{-10}	3.8×10^{-10}

$^{(a)}$ Assuming a distance of 10 kpc; $^{(b)}$ unabsorbed flux in unit of erg cm^{-1} s^{-1}.

and *INTEGRAL*/ISGRI data. The best fit to the data required a two-component model, a cutoff PL, or a thermal Comptonization model, together with a soft component, see Table 2. The hard spectral component contributes most of the observed flux (76%), even though a soft BB component is needed by the data. Observationally, the best-fit parameters are similar to those observed in BHC in their low/hard state (see e.g. Wilms et al., 2006) and in weakly magnetic neutron-star LMXB in their low-luminosity states (see e.g. Barret et al., 2000). In the low/hard or low-luminosity state hard X-ray components extending up to energies of a few hundred keV have been clearly detected in these systems. In NS systems, the hard spectrum is dominated by a PL-like component, with a typical slope of $\Gamma \sim 1.5-2.5$, which is followed by an exponential cutoff at energies often $\gtrsim$ 20 keV (see e.g., Barret et al., 2000), with some contribution from an additional soft thermal component, $kT_{\rm soft}$. In BH systems in their low/hard state, the slope is around $\Gamma \sim 1.5-1.6$, with a high-energy cutoff of a few dozen keV (see e.g., Wilms et al., 2006), while contribution from a soft thermal component is observable only when the interstellar absorption is not too high (see e.g., Frontera et al., 2001). The soft thermal emission, $kT_{\rm soft}$, could be associated to the radiation from the accretion disc either for a NS of BHC source. The PL is usually interpreted as Comptonization of seed photons in hot, optical-depth plasma. Using the COMPTT model, the hard spectrum is described by unsaturated Comptonization of soft seed photons, $kT_{\rm seed} \sim 0.4$ keV, in the hot $kT_{\rm e} \sim 11$ keV optically-thick $\tau \sim 3$ plasma.

An important parameter is the distance to the source. Its galactic coordinates are l_{II}=20.7, b_{II}=-14.5, therefore in the direction of the galactic bulge and substantially below the galactic plane. Were the source within the galactic plane, its distance would be rather small ($\sim$ 1.5 kpc for a thin disc); the derived absorption of $(1-2)\times10^{21}$cm^{-2} is compatible with the total galactic absorption in that direction as estimated from HI maps. Assuming a distance to the galactic center of 8 kpc and a bulge radius of 3 kpc, we conclude that the distance to Swift J1922.7-1716 is between 5 and 11 kpc. With these distance estimates, the unabsorbed 0.1–100 keV flux of (3.3–3.9)$\times10^{-10}$erg cm^{-2} s^{-1} (considering the different models) translates to a luminosity of (1–5)$\times10^{36}$ erg s^{-1}, compatible with both NS and BH sources at low accretion-rate levels. We assume the source is probably located in the galactic bulge. At the minimal distance of 5 kpc, the BB fits would imply an emission radius of only 3–4 km. This hints at a larger source distance. The radii obtained with the DBB fits are also very small and depend crucially on the inclination of the source. Using a mean inclination angle of 60° and a source distance of 10 kpc, an acceptable $R_{\rm in} \sim 13-18$ km can be obtained. We note that the distance estimates assume that the observed emission originates from the entire BB surface facing the observer. The presence of an obscuring structure, such as an accretion disc or stream, will affect those estimates.

We conclude that we observed Swift J1922.7-1716 in its hard state, during which it emits hard X-rays up to 100 keV. The soft excess, $kT_{\rm soft} \sim 0.4$ keV detected at low energies is most likely originating in the accretion disc. As for the hard component, it most likely originates in the Comptonization of soft seed photons, $kT_{\rm seed} \sim 0.53$ keV in a hot plasma. Our results are compatible with the soft emission being the source of the seed photons, i.e. $kT_{\rm soft} = kT_{\rm seed}$. From the best-fit spectral parameters and the timing properties, we cannot tell whether the objects harbors a NS or a BH. Interestingly, we could obtain a satisfactory fit with the same model as all three non-simultaneous spectra (*Swift*/XRT, *RXTE*/PCA, and *INTEGRAL*/ISGRI), indicating that its spectrum most likely remained constant if the source varied between the observations. Once again, this is a typical observational fact both in NS and BH systems at low luminosity. The measured $N_{\rm H}$ value is consistent with the expected Galactic value in the source direction Swift J1922.7-1716. This consistency suggests the absence of intrinsic absorption and, together with the position in the sky, indicates that it is most likely located in the Galactic bulge. The lack of iron-line emission is consistent with the absence of a reflected component in the broad band spectrum of the source. The fact that Swift J1922.7-1716 was not detected in the ISGRI data from March 2003 to October 2004, for a total 20–60 keV exposure time of 420 ks, indicates that the system is either very variable on long time scales or transient. Across the period spanned by our observations (2005 July to October), both flux level and spectrum were compatible with being constant.

Acknowledgements. We are grateful to G. L. Israel for support for the search for coherent pulsations. MF acknowledge the French Space Agency (CNES) for financial support. TB and SG acknowledge support from ASI grants I/R/046/04 and I/023/05/0.

References

Arnaud, K. A. 1996, in Astronomical Data Analysis Software and Systems V. ed. G. H. Jacoby, & J. Barnes, ASP Conf. Series 101 (San Francisco: ASP), 17

Barret, D., Olive, J. F., Boirin, L., et al. 2000, ApJ, 533, 329

Belloni, T., Psaltis, D., & van der Klis, M. 2002, ApJ, 572, 392

Belloni, T., Colombo, A. P., Homan, J., et al. 2002, A&A, 390, 199

Dickey, J. M., & Lockman, F. J. 1990, Annu. Rev. A&A, 28, 215

Frontera, F., Zdziarski, A. A., Amati, L., et al., 2001, ApJ, 561, 1006

Goldwurm, A., Daid, P., Foschini, L., et al. 2003, A&A, 411, L223

Gros, A., Goldwurm, A., Cadolle-Bel, M., et al. 2003, A&A, 411, L179

Israel, G. L., Stella, L. 1996, ApJ, 468, 369

Jahoda, K., Swank, J. H., Giles, A. B., et al. 1996, Proc. SPIE, 2808, 59

Lebrun, F., Leray, J.-P., Lavocate, Ph., et al. 2003, A&A, 411, L141

Lund, N., Budtz-Joergensen, C., Westgaard, N. J., et al. 2003, A&A, 411, L231

Mitsuda, K., Inoue, H., Koyama K., et al. 1984, PASJ, 36, 741

Rothschild, R. E., Blanco, P. R., Gruber, D. E., et al. 1998, ApJ, 496, 538

Titarchuk L., 1994, ApJ, 434, 570

Tueller, J., Barthelmy, S., Burrows, D., et al. 2006, Astr. Tel., 668

Tueller, J., Barthelmy, S., Burrows, D., et al. 2006, Astr. Tel., 669

Ubertini, P., Lebrun, F., Di Cocco, G., et al. 2003, A&A, 411, L131

Wilms, J., Nowak, M.A., Pottschmidt, K., Pooley, G.G., Fritz, S., 2006, A&A, 447, 245

Winkler, C., Courvoisier, T. J.-L., Di Cocco, G., et al. 2003, A&A, 411, L1